JACS
JOURNAL OF THE AMERICAN CHEMICAL SOCIETY
Article
pubs.acs.org/JACS

Proline Primed Helix Length as a Modulator of the Nuclear Receptor−Coactivator Interaction

Sascha Fuchs,[†,‡] Hoang D. Nguyen,[†,§,‡] Trang T. P. Phan,[§] Matthew F. Burton,[†] Lidia Nieto,[†] Ingrid J. de Vries-van Leeuwen,[†] Andrea Schmidt,[†] Monireh Goodarzifard,[†] Stijn M. Agten,[†] Rolf Rose,[§] Christian Ottmann,[†,§] Lech-Gustav Milroy,[†] and Luc Brunsveld*[,†,§]

[†]Laboratory of Chemical Biology, Department of Biomedical Engineering, Technische Universiteit Eindhoven, Den Dolech 2, 5612 AZ Eindhoven, The Netherlands

[§]Chemical Genomics Centre of the Max Planck Society, Otto-Hahn Straße 15, 44227 Dortmund, Germany

Supporting Information

ABSTRACT: Nuclear receptor binding to coactivator proteins is an obligate first step in the regulation of gene transcription. Nuclear receptors preferentially bind to an LXXLL peptide motif which is highly conserved throughout the 300 or so natural coactivator proteins. This knowledge has shaped current understanding of this fundamental protein−protein interaction, and continues to inspire the search for new drug therapies. However, sequence specificity beyond the LXXLL motif and the molecular functioning of flanking residues still requires urgent addressing. Here, ribosome display has been used to reassess the estrogen receptor for new and enlarged peptide recognition motifs, leading to the discovery of a potent and highly evolved PXLXXLLXXP binding consensus. Molecular modeling and X-ray crystallography studies have provided the molecular insights on the role of the flanking prolines in priming the length of the α-helix and enabling optimal interactions of the α-helix dipole and its surrounding amino acids with the surface charge clamp and the receptor activation function 2. These findings represent new structural parameters for modulating the nuclear receptor−coactivator interaction based on linear sequences of proteinogenic amino acids and for the design of chemically modified inhibitors.

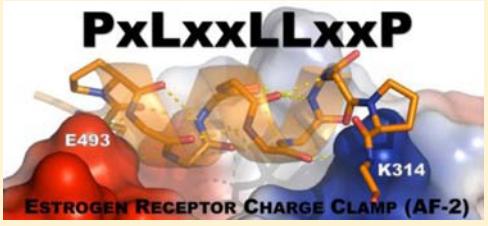

INTRODUCTION

Nuclear receptors (NR) are a superfamily of ligand-activated gene transcription factors[1] important for a host of critical physiological processes including embryonic development, reproduction, as well as for the malignant course of multiple diseases including cancer.[2] Indeed, overexpression of the estrogen receptor (ER) and the upregulation of ER signaling are primary causes of breast cancer.[3] Modulating ER-mediated gene transcription through the use of anti-estrogens, small lipophilic drug molecules that directly target the ligand-binding pocket (LBP), has been the most successful approach to date for the pharmacological treatment of breast cancer. This has included the ground-breaking development of 'selective estrogen receptor modulators',[4] or SERMS, for example tamoxifen,[5] which manage improved cell and tissue selectivity through a more discriminant recruitment of coactivator proteins. Nevertheless, there is an ongoing demand for more selective ER modulators operating through novel mechanisms of action.[6]

As an alternative to classical anti-estrogens, competitive inhibition of the ER−coactivator interaction has emerged as a promising therapeutic strategy, ably assisted by a growing knowledge of the molecular parameters of NR coactivator binding.[1] In the classical case, ligand binding at the LBP induces a conformational change, most prominent in the mobile helix 12 (H12) region, which favors binding of an α-helical LXXLL consensus motif to the NR's ligand binding domain (LBD).[7] A defining feature of this interaction is the 'charge clamp', formed at the interface between H12 and other parts of the activation function 2 (AF-2), which binds coactivators via a short α-helix of precise length.[8] This feature positions the NR−coactivator interaction uniquely among other α-helix mediated protein−protein interactions that are typically characterized by longer α-helical segments that do not require the additional electrostatic stabilization of a charge clamp.[9−12] This specific design feature offers a unique opportunity for the development of selective inhibitors. Seminal work on the phage display screening of large LXXLL-derived peptide libraries identified potent and selective ER−coactivator inhibitors.[13−16] This has motivated recent efforts to develop small lipophilic drug-like molecules which target the surface charge clamp or which mimic the leucine side chains of the coactivator α-helix, either via computational design[17,18] or using high-throughput screening methods.[19−23] Indeed, potent peptide binders with enhanced helical propensity have been developed using macrocyclization strategies based on either disulfide bond bridging,[24,25] macrolactamization[26] or hydrocarbon stapling.[27] In a number of cases,

Received: December 2, 2012
Published: February 26, 2013

   dx.doi.org/10.1021/ja311748r | J. Am. Chem. Soc. 2013, 135, 4364−4371

this has resulted in peptide binders with impressive binding affinities, ER subtype selectivity and proteolytic stability. However, given that these examples have built on prior knowledge of natural coactivators or peptide sequences derived from phage display screening (and are therefore restricted to the inherent diversity of the systems at hand), it was not clear that a consensus had been reached on the minimal structural requirements for potent coactivator binding using only natural amino acids.

Here, we describe the use of ribosome display[28−30] to effectively screen the ER surface for novel peptide binders. The ability of this approach to sample a significantly larger and more diverse peptide pool[31] facilitates a closer examination of the LXXLL flanking regions than has previously been possible, and the opportunity to uncover entirely new peptide motifs. In this work, initial rounds of ribosomal enrichment witnessed the emergence of the same LXXLL consensus identified by phage display screening. Intriguingly, though, further rounds of enrichment produced a more evolved PXLXXLLXXP motif, most prominent for ERβ, which gave rise to a series of potent peptide sequences. The most promising sequences were investigated in biochemical and cell-based assays as mEGFP peptide−protein fusions or synthetic peptides using solid-phase peptide synthesis (SPPS). Results from follow-up molecular modeling and X-ray co-crystallography studies defined a clear role for the flanking prolines as 'helix primers', thus priming the helix length for optimal recognition of the helix dipole by the charge clamp. Additionally, the proline residues impose conformational constraints on flanking amino acids, restricting their orientation and stabilizing H-bonding interactions through a possible increase in hydrophobicity at the charge clamp. This has resulted in the rational design of potent proline peptide inhibitors consisting only of natural amino acids and has set the stage for the future development of peptide-derived tools, genetically encoded cellular inhibitors and drug therapies.

RESULTS

Design and Execution of Ribosome Display Screening. A randomized DNA library with a theoretical size of 1.1×10^{15} was cloned into a plasmid for evaluation against both ERα and ERβ. Figure 1a shows an overview of the library design (see as well the Supporting Information). The central amino acid of the otherwise randomized region was fixed to arginine (R), serving as a molecular ruler that restricts the number of consensus motif positions possible within the random sequence. Strikingly for ERβ, a consensus PXLXXLL motif was already evident after four rounds of ribosomal enrichment, and sequencing and cluster analysis of intermediate sequences (Figure 1b). This rapidly became PXLXXLLXXP through rounds six and eight. The emergence of the same PXLXXLLXXP motif was also witnessed for ERα, but only during the later stages of ribosomal screening, and to a lesser extent than for ERβ. Sequence analysis after round eight thus identified 24 and 40 novel peptides sequences, for ERα and ERβ, respectively. Nine peptides (Figure 1c, **2**−**10**) were selected for further biochemical studies into the PXLXXLLXXP consensus motif. A comprehensive list of ribosome-derived peptide sequences can be found in the Supporting Information.

Preliminary Validation of Ribosome Hits. A preliminary screen of peptides **2**−**10** (as mEGFP protein−peptide fusions) in a fluorescence polarization (FP) assay (Figure 2a) served to validate their ER binding properties. Data from mammalian two-hybrid (Figure 2b and Supporting Information) and

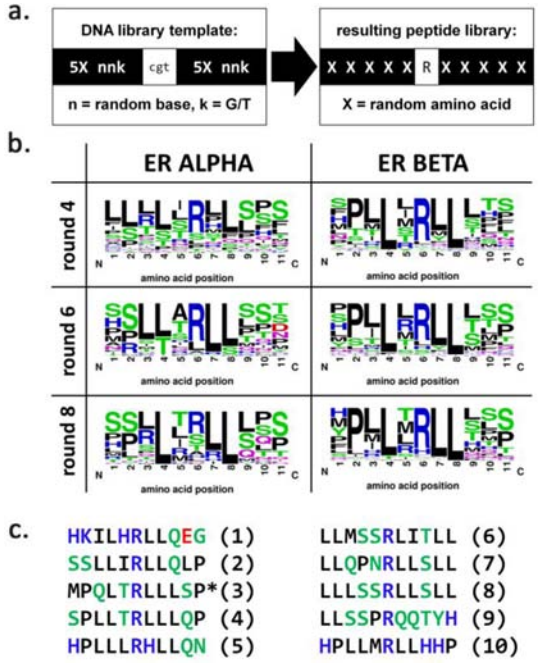

Figure 1. Ribosome display screening of the ER surface. (a) Design of peptide library (Supporting Information); (b) sequence cluster analysis of peptide hits for ERα and ERβ through rounds four, six and eight, manually refined to account for multiple LXXLL registers. Amino acid color coding: blue, positively charged; red, negatively charged; green and magenta, polar; black, hydrophobic. (c) LXXLL aligned sequences: naturally derived NCoA-1 Box 2 sequence, **1**, and peptide sequences **2**−**10** identified after round eight of ribosome display screening (a full list of ribosome display peptides can be found in the Supporting Information).

cellular competitive inhibition studies of the most promising sequences not only reinforced the preliminary FP data, but also suggested that the proline peptides are significantly more potent inhibitors of coactivator binding in a cellular setting compared with the natural sequence NCoA-1, **1** (Figure 2d,e). This activity trend makes sense in light of work by McDonnell et al. on phage display peptides, where double LXXLL motifs were required to achieve a similarly efficacious blocking of gene transcription.[14] Cluster analysis data (Figure 1b) combined with the preliminary data suggested that the flanking prolines in particular determine the improved binding properties of the proline peptides (compared with **1**, which lacks flanking prolines). To investigate this further, the most potent peptides, **4**, **5** and **10** (Table 1), were synthesized by solid-phase peptide synthesis (SPPS) using standard techniques (Supporting Information).

Amino Acid Exploration of PXLXXLLXXP Motif Using Synthetic Peptides. The ERβ binding affinities were measured in a competition fluorescence polarization assay (Table 1 and Supporting Information). K_i values were calculated using the experimentally derived K_d value for the competitor peptide, fluorescein (FAM)-labeled NCoA-1 (FAM-**1**). Overall, the peptides afforded classical sigmoidal curves and functioned as competitive inhibitors with K_i values in the 0.025−75 μM range. Sequences **4**, **5** and **10** (each measuring K_i < 0.050 μM) were stronger binders than **1** (K_i = 0.122 μM). In general, truncation of peptide sequences **4** and **10** resulted in a loss in binding affinity (Table 1). For example, N-terminal truncation of 19-mer **4** yielded a peptide (15-mer

dx.doi.org/10.1021/ja311748r | J. Am. Chem. Soc. 2013, 135, 4364−4371

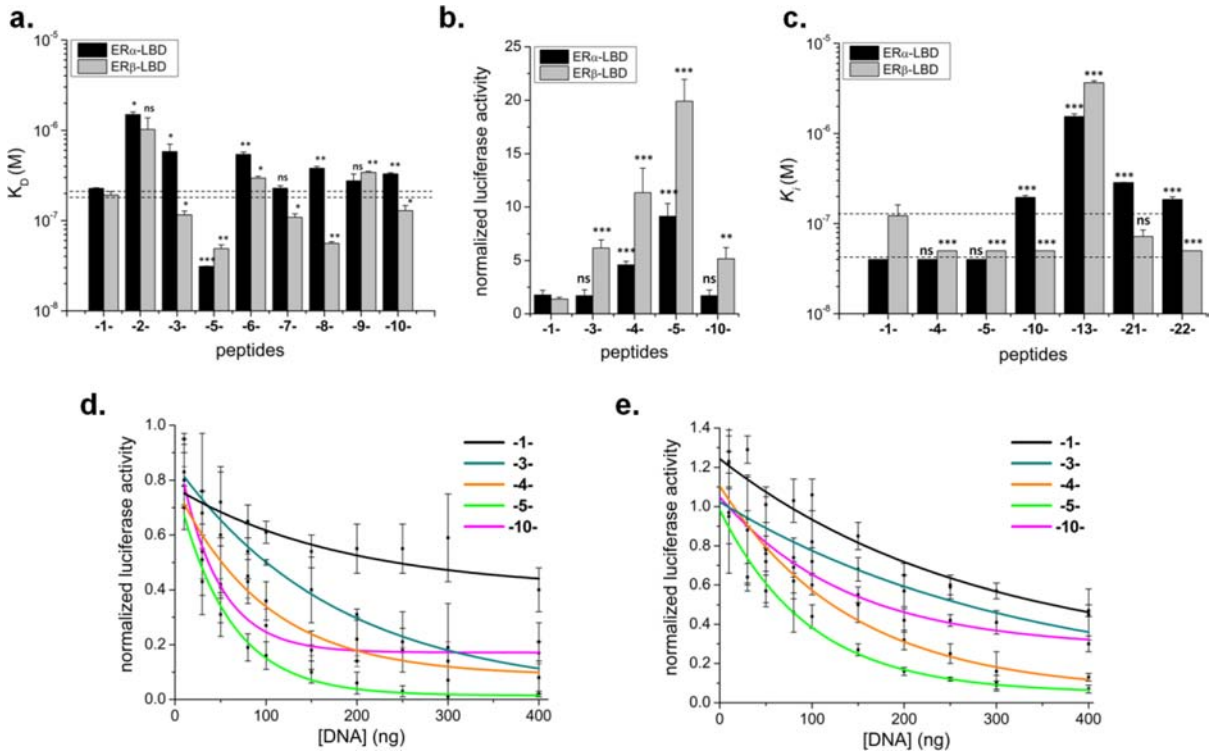

Figure 2. Validation of peptide sequences identified by ribosome display screening against ERα and ERβ. (a) Comparison of the K_d values (mean ± SEM) of peptides **1**–**10** as mEGFP-peptide fusions as determined by a binding fluorescence polarization assay (Supporting Information). (b) Comparison of luciferase activity (mean ± SEM) for peptide sequences **1**, **3**–**5**, and **10** in a mammalian-two hybrid assay in U2OS cells, ERα-(black), ERβ-LBD (gray). (c) Comparison of peptide **1**, **4**, **5**, **10**, **13**, **21** and **22** K_i values (mean ± SEM) for binding to ERα and ERβ determined in a competitive fluorescence polarization assay (see Table 1 for all ERβ values and Supporting Information for all ERα values). The dashed lines facilitate comparison of peptide activities with the reference peptide (**1**, n = 5; others, n = 3). Comparison of luciferase activity (mean ± s.e.m.) for peptides **1**, **3**–**5** and **10** (normalized against sample without inhibitor peptide) in a cellular competitive inhibition assay against ERα (d) and ERβ (e).

Table 1. Biochemical Characterization of Peptides for ERβ Derived from a Competitive Fluorescence Polarization (FP) Assay versus FAM-Labeled 1

Peptide sequence[a]	No.	IC_{50} / μM (±)[b]	K_i / μM (±)[b]
LTERHKILHRLLQEGSPSD	**1**	0.470 (0.059)	0.122 (0.039)
LTARSPLLTRLLLQPSPSD	**4**	0.171 (0.009)	< 0.050 (-)
LTARHPLLLRHLLQNSPSD	**5**	0.184 (0.044)	< 0.050 (-)
LTARHPLLMRLLHHPSPSD	**10**	0.279 (0.028)	< 0.050 (-)
SPLLTRLLLQPSPSD	**11**	0.466 (0.040)	0.119 (0.026)
HPLLMRLLHHPSPSD	**12**	7.15 (0.85)	4.62 (0.25)
HPLLMRLLHHPS	**13**	5.38 (0.61)	3.64 (0.21)
EPILHRLLQKP[c]	**14**	38.4 (17.9)	25.7 (12.1)
SPILHRLLQEP[c]	**15**	n.b. (-)	n.b. (-)
RHKPLHRLLQEPS[c]	**16**	98.2 (12.5)	66.0 (8.4)
RHPILHRLLQPEG[c]	**17**	2.83 (0.12)	1.71 (0.08)
RHPLHRLLQEAPS[c]	**18**	112.1 (17.6)	75.4 (11.9)
RHPKILHRLLQPE	**19**	1.46 (0.10)	0.787 (0.066)
PILHRLLQEP[c]	**20**	0.680 (0.102)	0.262 (0.068)
HPILHRLLQEP[c]	**21**	0.395 (0.020)	0.072 (0.013)
HPLLMRLLLSP[c]	**22**	0.132 (0.020)	0.025 (0.015)
HPLLMRLLLSP	**23**	0.289 (0.017)	< 0.050 (-)
HKILHRLLQEG[c]	**24**	0.591 (0.120)	0.203 (0.080)
KILHRLLQEG[c]	**25**	0.695 (0.144)	0.272(0.096)

[a]See the Supporting Information for details of peptide synthesis and determination of K_i values; LXXLL motif highlighted in gray, flanking prolines in red bold. [b]± sign is a standard error (SEM). [c]N-terminally acetylated; n.b., no binding detected.

11) which was at least 2.5 times less potent than the parental peptide, while 15-mer **12**, an N-terminally truncated analogue of 19-mer **10**, was also significantly less potent. Subsequent C-terminal truncation of **12** yielded 12-mer **13**, without any significant change in activity (K_i = 3.6 μM). This data highlights the fact that the flanking regions of the LXXLL motif can contribute to ER binding, and that the presence of the proline residues alone is not per definition sufficient for potent binding. Interestingly though, insertion of the two proline residues into the NCoA-1 derived 11-mer peptide **21** generated a more active binder (compare with **24**, Table 1). As further evidence of the strength of ribosome display screening to select the most active sequences, a consensus 11-mer peptide consisting of the most frequent amino acids to emerge from the ERβ screen (Figure 1b) furnished the strongest ERβ inhibitor of the series (K_i = 0.025 μM, **22**, Table 1). A selection of the most interesting analogues was also tested against ERα in the same fluorescence polarization assay (Figure 2c and Supporting Information). In line with expectations,[32] **1** bound with greater affinity to ERα than ERβ. However, with the exception of analogue **13**, all proline peptides tested against both isoforms were either equally active or more selective for ERβ; with the highest ERβ selectivity observed for analogues **10** and **21**-**22** (Figure 2c). This selectivity is reflected in the more prominent and earlier emergence of the prolines in the presence of ERβ during ribosomal display screening (Figure 1). Synthetic mutations were also introduced to investigate the influence of charge and the repositioning of the proline residues relative to

dx.doi.org/10.1021/ja311748r | J. Am. Chem. Soc. 2013, 135, 4364–4371

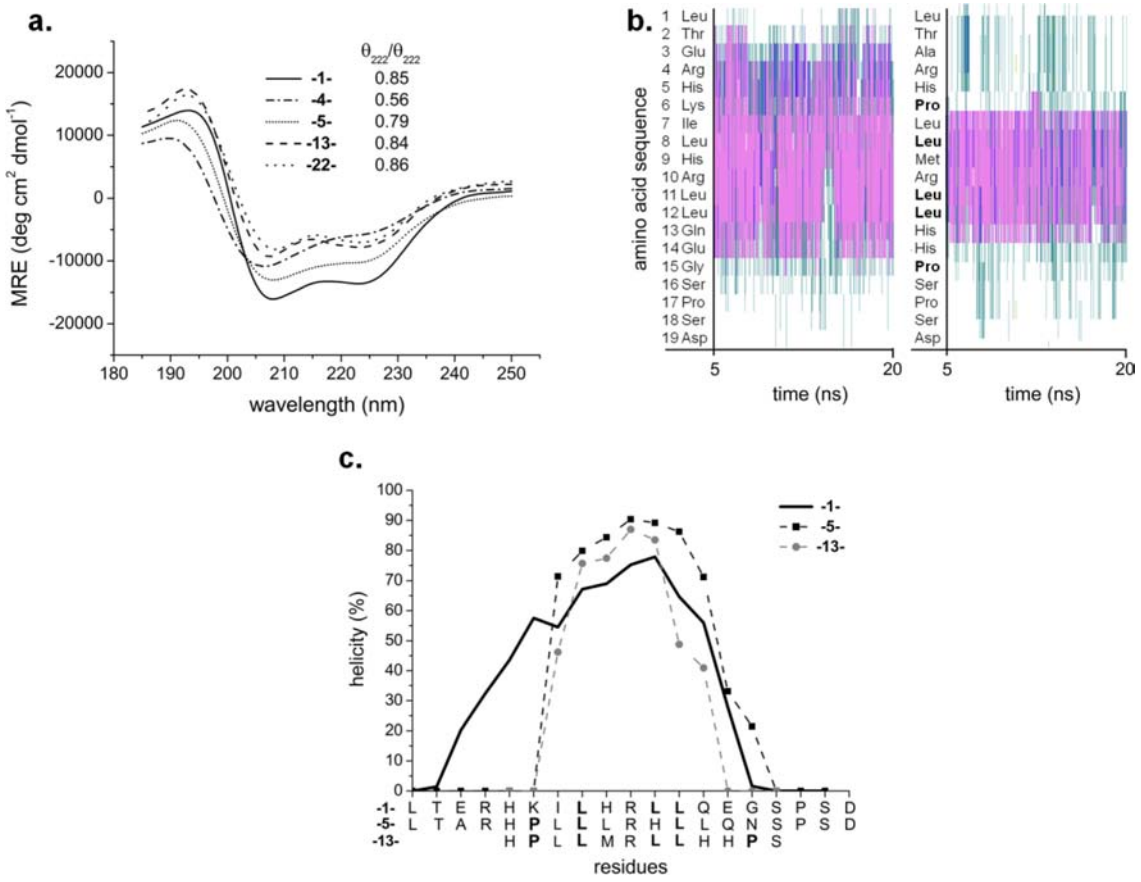

Figure 3. Structural analysis of proline-derived peptide binders. (a) Comparison of circular dichroism (CD) data for peptides **1**, **4**, **5**, **13** and **22** (Table 1), 5 mM sodium phosphate buffer, pH 7.4 with 30% TFE (v/v) (see Supporting Information for circular dichroism (CD), experimental, and all spectra). (b) Secondary structure vs time plot of peptide **1** (left) vs proline peptide **10** (right): pink (α-helix), blue (3_{10}-helix), green (turn), white (unordered). For the lowest-energy conformation of all peptides after 20 ns MD simulation see the Supporting Information. (c) Averaged % helicity vs peptide sequence derived from a 20 ns molecular dynamics simulation: comparison of peptides **1**, **5** and **13**. The degree of helical content per residue was obtained using the *ptraj* module of AMBER (omitting the first 5 ns of each simulation).

the core LXXLL motif (Table 1). For example, modifying the charge of amino acids adjacent to the proline residues abolished activity (Table 1, compare **14** and **15**). 'Shunting' of the proline residues in the direction of the LXXLL motif caused activity to diminish, more so at the N-terminus than at the C-terminus (Table 1, compare **16**, **17** and **18**), thus suggesting that the position and charge environment of Pro-2 are optimally expressed within the consensus motif. Truncated synthetic peptides were acetylated at the N-terminus to neutralize the effects of charge on binding. On the basis of the results for **22** and **23** in Table 1 (where N-terminal acetylation can be directly assessed), acetylation was shown to enhance binding affinity (IC_{50} = 0.132 vs 0.289 μM). Acetylation overcomes unfavorable interactions between the positively charge N-terminus (at low or neutral pH) and the helix dipole and can stabilize helix formation through an additional hydrogen bond at the acetyl carbonyl group.[33] Collectively, the data shows that prolines residues, when optimally located in the flanking regions of the core LXXLL motif, contribute significantly to peptide binding at the ER surface.

Structural Basis for the Potent Binding of the Proline Peptides. Circular dichroism (CD) measurements were made to determine the secondary structure of the peptides (Figure 3a, Supporting Information). In phosphate buffer, the addition of 30% (v/v) trifluoroethanol (TFE), reported to stabilize intramolecular hydrogen bonds and mimic the environment at the protein surface,[34] strongly induced α-helix formation in nearly all cases, suggesting that the proline peptides become strongly helical at the NR surface. Molecular dynamics (MD) simulations reinforced this view (Figure 3b,c and Supporting Information), and in addition identified a specific role for the flanking prolines in determining the helix length. Comparison of secondary structure versus time for **1** and **10** (Figure 3b) clearly highlights the effect of the two prolines on limiting the helix to precisely the length required to bind to the charge clamp (vide infra). This shortening of the helix length does not compromise, and in some cases stabilizes, the helical stability of the LXXLL segment (e.g., Figure 3c).

To gain structural insight into the significance of the flanking prolines within the peptide−protein complex, the X-ray structures of peptides **5** and **13** were co-crystallized with the ERβ ligand binding domain (LBD) (Figure 4 and Supporting Information). For peptide **13** (Figure 4a), the flanking prolines are located above the charge clamp residues: glutamic acid at position 493 (E493) and lysine at position 314 (K314) (Figure 4b), respectively.

An overlay of the X-ray cocrystal structures of **1** and **5** (Figure 4c), both expressing a histidine residue (His) at the −3 position, revealed that the Pro-2 in **5** assists in directing the His side chain residue toward E493 and an additional glutamic acid residue, E332, located at the ER surface, thereby forming an additional hydrogen-bonding interaction motif. Similar obser-

dx.doi.org/10.1021/ja311748r | J. Am. Chem. Soc. 2013, 135, 4364−4371

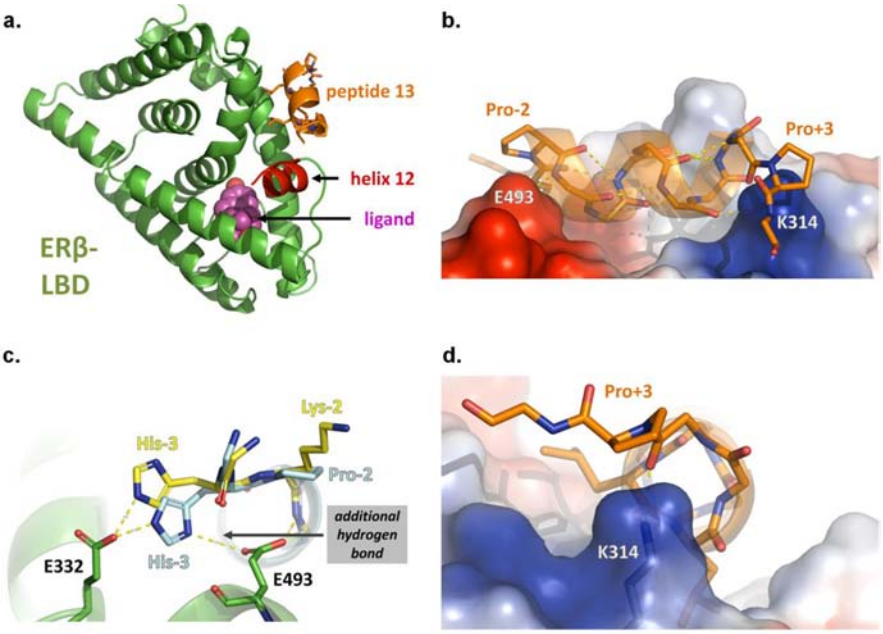

Figure 4. X-ray crystallography analysis of the proline peptides. (a) Overview of co-crystal structure of peptide **13** (orange) with the ligand-bound (17β-estradiol, E2, purple) estrogen receptor β (ERβ)-ligand binding domain (LBD) (green). The helix 12 is colored red. (b) Close-up of **13** (carbon atoms colored orange) bound to ERβ LBD. The protein surface is colored red and blue to highlight the charge clamp residues E493 and K314. The flanking prolines delineating the α-helix length are labeled Pro-2 and Pro+3. (c) Superimposition of the N-terminal region of the co-crystal structures of peptides **1** (yellow, NCoA-$1_{683-701}$, PDB accession code: 3ols) and **5** (light blue) bound to the ERβ-LBD, showing the additional hydrogen bond of the histidine of **5**. (d) Close-up of the C-terminal region around charge clamp residue K314 of peptide **13** bound to the ERβ-LBD (see Supporting Information for X-ray diffraction data and stereo images of a portion of the electron density map).

vations were made for the ERβ co-crystal structure with **13**. Moreover, MD simulations in explicit solvent showed that these additional hydrogen bonds are extraordinarily stable throughout the 6-ns simulation (Supporting Information). Our data would suggest that the histidine-proline motif (HPX) stabilizes peptide binding and thus contributes to higher binding affinities. For example, scission of the His residue preceding Pro-2 in peptide **21** (to give **20**) brought about a 3-fold loss in inhibitory activity (Table 1, K_i = 0.072 μM with respect to K_i = 0.262 μM), thus supporting the structural observations. In contrast, removal of His-3 from an 11-mer derived from the natural NCoA-1 sequence, not flanked by a proline but a lysine, did not cause any statistically significant change in the K_i value (Table 1, **24** with respect to **25**). Clearly though, the major contribution made by the prolines to the overall binding affinity of the peptide is in determining the precise helix length and optimal helix dipole interaction with the charge clamp. Taken together, the MD calculations and X-ray crystallography data, provide convincing evidence of the influence of the prolines, acting as a molecular ruler, in determining helix length in the surface bound state.

As further confirmation of the superior binding properties of the proline derived peptides, mammalian two-hybrid studies were performed on peptides **1**, **21** and **22** and point mutants of **1** bearing systematically inserted flanking proline residues (**1*** and **1****) (Figure 5). Whereas all five peptides were as active toward ERα (Figure 5a), variants **21**, **22** and **1*** were substantially more active toward ERβ than **1**. Interestingly, peptide **22** retained significant activity in the absence of 17β-estradiol (E2). This result might indicate E2 independent regulation of gene transcription as a unique feature of the proline derived peptides. Furthermore, mutant **1**** was notably less potent than **1*** (and only slightly more active than **1**), suggesting here that Pro-2 contributes more than Pro+3 to the added binding properties of the proline peptides. Mutant studies were also performed to cross-examine the hydrogen-bonding interaction between His-3 and the charge clamp residue E493 (Figure 5b). For ERβ, mutation of the charge clamp Glu residue to Ala (E493A) resulted in a dramatic loss in binding affinity for **1**, **21**, **1*** and **1****. Interestingly for ERα, however, both peptides **1** and **1**** (without Pro-2) showed significant binding to both the mutant (E542A) as well as the wild type (Figure 5b). The results indicate the subtle interplay and importance of the backbone directed orientation of side-chains for ER binding and for engineering receptor subtype selectivity using natural amino acids.

The coordinates of the protein–ligand crystal structures have been deposited at the Protein Data Bank with the following PDB IDs: ERß-**5** (4J24); ERß-**13** (4J26).

■ DISCUSSION

Functional LXXLL motifs are not exclusive to NR coactivators, having also been identified in other transcription factors, including the calcium response element binding (CREB)-protein (CBP), p300, and other mediator subunits.[35] Indeed, nature makes frequent use of leucine rich α-helical structures for a variety of purposes including, the HIV-1 accessory protein Vpr,[36] and leucine zipper proteins such as c-jun/c-fos.[37] In contrast to transmembrane proteins such as GPCRs, where they introduce functional kinks or perturbations into long α-helical structures,[38] prolines are more frequently located at the termini of α-helices in water-soluble proteins. There, they form N- and C-capping motifs,[39−41] which contribute to helix stability and the specificity of protein folding through the correct positioning of adjacent side-chain residues.[42] The proline peptides characterized in this present work behave as

dx.doi.org/10.1021/ja311748r | J. Am. Chem. Soc. 2013, 135, 4364−4371

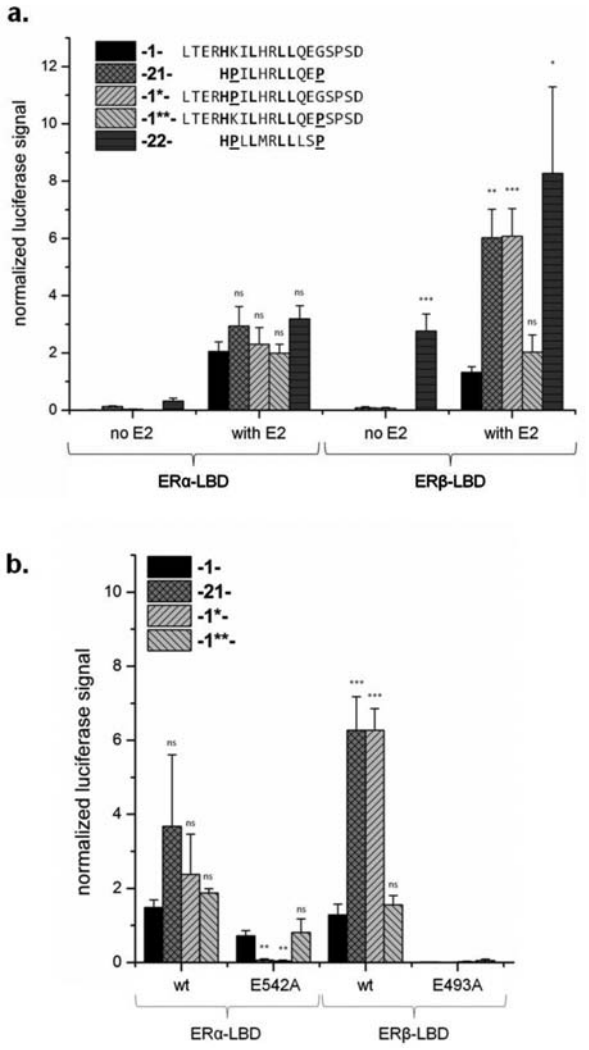

Figure 5. Mammalian two-hybrid studies on peptides **1**, **21** and **22** comparing normalized luciferase activity (mean ± SEM) for ERα vs ERβ. The NCoA1-Box 2 mutants with one proline residue at either the −2 (**1***) or +3 positions (**1****) were also included: (a) with and without 17β-estradiol (E2), and (b) wild-type (wt) vs ER charge clamp mutants E378A and E542A, respectively (n = 3).

such soluble proteins. The molecular dynamics (MD) simulations and circular dichroism (CD) data[43] suggest that the peptide segment between the two prolines becomes helical under conditions that mimic the close proximity of the protein environment. According to classical Zimm−Bragg[44] and Lifson-Roig[45] helix−coil transition theory, the strong helical propensity of the proline peptides is dictated by the core LXXLL motif, where the leucine residues function to nucleate the formation and propagation of the α-helix, while the helix averse proline residues determine helix length.[46] The LXXLL coactivator motif was initially thought to function solely as a docking module.[47] Later, phage display screening of the flanking regions indentified three distinct extended recognition motifs.[14] Indeed, PXLXXLL was identified as one of those three peptide classes. However, only four examples were cited in this case (one of which showed an interesting selectivity for ERβ over ERα). In a separate piece of work, diverse recombinant peptide libraries were simultaneously screened against ERβ and TRβ.[16] As for ERα in the previous example, only a few of the ERβ-specific peptide sequences identified in this case (three of 19) contained a proline residue at the −2 position. PXLXXLL has also been identified as a binding motif specifically for PPAR[48] and MR.[49]

Thus the emergence of the flanking prolines through multiple rounds of ribosomal enrichment is symptomatic of the fact that the surface charge clamp binds α helices of a precise length.[24,50] The improved binding and inhibitory activity observed for the proline peptides (compared with the natural sequence **1**) is believed to originate for two reasons. The first and main reason is to minimize the entropic penalty by ensuring the correct helix length and by optimizing the electrostatic interaction between the helix dipole and the surface charge clamp. It could be hypothesized that the relatively hydrophobic proline residues, in their precise location above the two charge clamp residues (Figure 4), shield the charge clamp residues from solvent, thereby strengthening the electrostatic interaction. A related more subtle reason is postulated whereby the conformationally constrained proline residues facilitate additional, stabilizing hydrogen bond interactions (e.g., with E493 for ERβ), dictated by the increased hydrophobicity. Indeed, the unique combination of conformational rigidity and hydrophobicity make proline ideally suited for protein−protein interactions operating via short peptide sequences.[51] That said, while the activities of the proline peptides reached in this present study compare favorably with previously reported peptide-based ER coactivator inhibitors (see the Supporting Information for data comparison),[24−27] further manipulation of the NR Box should in the future address improved affinity and NR selectivity.[26,50] For example, Guy and Geistlinger demonstrated NR and isoform selective inhibition through subtle chemical variation of the leucine side-chains of a macrolactam modified peptidomimetic derived from NCoA-2 (Supporting Information). In one instance, replacing one of the leucine side-chains with a *o*-chlorophenyl substituent group resulted in ERβ selective inhibition over ERα in the presence of 17β-estradiol.[26,52] Thus, it is the integration of high throughput screening methods such as the ribosome display screening presented in this work combined with structure−activity relationship studies of non-natural peptide analogues[24−27] that will most likely lead to success in the design of potent inhibitors.

On current evidence, it could be further speculated that coactivator proteins bearing proline residues in the flanking regions of the LXXLL serve a specific evolutionary function. For example, as with electrostatic interactions (e.g., at the surface charge clamp) and the use of hydrophobic consensus motifs (e.g., LXXLL), proline-primed helix length may have evolved as a regulator of the NR targeting of specific coactivator proteins: for example, the two NR boxes of TRAP220/MED1 both with prolines located at the −2 position (NPILTSLLQ and HPMLMNLLK),[53,54] as well as NF-κB inhibitor beta (NPILARLLR)[55] and NCoA-6/ASC-2 (SPLLVNLLQ).[56,57] Even so, proline residues are rarely found in the flanking regions of natural coactivator sequences (compare Figure 1b with Figure S11 in the Supporting Information). This may be because the proline peptides bind too strongly, e.g., ligand independent (**22**, Figure 5a), and indiscriminately to be useful for NR-coactivator signaling, which typically operates via weaker more transient protein−protein interactions. The selectivity of the proline peptides reported in this work is currently being investigated toward other NRs, and we can so far report significant activity toward the retinoid X receptor

dx.doi.org/10.1021/ja311748r | J. Am. Chem. Soc. 2013, 135, 4364−4371

(Supporting Information), suggesting that proline-derived peptide sequences are useful for targeting other NRs.

CONCLUSIONS

In conclusion, a novel use of ribosome display has been described, which effectively screens the ER surface for novel peptide binders. In this way, a series of proline peptide sequences were discovered conforming to a highly evolved PXLXXLLXXP consensus motif. On the basis of biochemical and X-ray crystallography data, the proline residues are shown to optimize helix binding to the surface charge clamp by determining the precise helix length. Furthermore, the proline residues increase the hydrophobicity at the charge clamp residues, which strengthens the electrostatic interactions and favors more stabilizing hydrogen bond interactions. Finally, the proline-derived peptides represent a set of minimal structural parameters, providing defined secondary structure boundaries, for regulating the ER−coactivator interaction, based exclusively on natural amino acids and without recourse to additional chemical modifications. This work has thus provided fundamental molecular insights into the regulation of these protein−protein interactions, potentially transferable to other protein−protein interactions, and laid important foundations for the future development of peptide-derived tools and peptide-derived drug approaches.

ASSOCIATED CONTENT

Supporting Information

Details of the ribosome display screening, including an overview of the screening protocol, the oligonucleotides used, the design of the ribosome library and a list of all ribosome peptide sequences; biochemical and cellular characterization of the peptide sequences, including fluorescence polarization assay, far-UV circular dichroism spectroscopy (for ERα and ERβ) and mammalian two-hybrid studies; solid phase peptide synthesis, including characterization of the final peptides; molecular dynamics simulations, X-ray crystallography and statistical analysis of data. This material is available free of charge via the Internet at http://pubs.acs.org.

AUTHOR INFORMATION

Corresponding Author

l.brunsveld@tue.nl

Author Contributions

‡S.F. and H.D.N. contributed equally.

Notes

The authors declare no competing financial interest.

ACKNOWLEDGMENTS

This work was supported in part by Bayer pharma, Merck-Serono, and Merck. The authors thank A. Visser (Merck) and P. Donner (Bayer-Schering-Pharma AG) for provision of plasmids and S. Möcklinghoff for help with initial protein crystallography.

REFERENCES

(1) Huang, P.; Chandra, V.; Rastinejad, F. *Annu. Rev. Physiol.* **2010**, *72*, 247−272.
(2) O'Malley, B. W.; Kumar, R. *Cancer Res.* **2009**, *69*, 8217−8222.
(3) Roy, S. S.; Vadlamudi, R. K. *Int. J. Breast Cancer* **2012**, 1−8.
(4) Smith, C. R.; O'Malley, B. W. *Endocr. Rev.* **2004**, *25*, 45−71.
(5) Uray, I. P.; Brown, P. H. *Expert Opin. Invest. Drugs* **2006**, *15*, 1583−1600.
(6) Moore, T. W.; Mayne, C. G.; Katzenellenbogen, J. A. *Mol. Endocrinol.* **2010**, *24*, 683−695.
(7) Nagy, L.; Schwabe, J. W. R. *Trends Biochem. Sci.* **2004**, *29*, 317−324.
(8) Li, Y.; Lambert, M. H.; Xu, H. E. *Structure* **2006**, *11*, 741−746.
(9) Davis, J. M.; Tsoub, L. K.; Hamilton, A. D. *Chem. Soc. Rev.* **2007**, *36*, 326−334.
(10) Jochim, A. L. J.; Arora, P. S. *Mol. BioSyst.* **2009**, *5*, 924−926.
(11) Jochim, A. L. J.; Arora, P. S. *ACS Chem. Biol.* **2009**, *5*, 919−923.
(12) Edwards, T. A.; Wilson, A. J. *Amino Acids* **2011**, *41*, 743−754.
(13) Paige, L. A.; Christensen, D. J.; Grøn, H.; Norris, J. D.; Gottlin, E. B.; et al. *Proc. Natl. Acad. Sci. U.S.A.* **1999**, *96*, 3999−4004.
(14) Chang, C.; Norris, J. D.; Grøn, H.; Paige, L. A.; Hamilton, P. T.; et al. *Mol. Cell. Biol.* **1999**, *19*, 8226−8239.
(15) Hall, J. M.; Chang, C. Y.; McDonnell, D. P. *Mol. Endocrinol.* **2000**, *14*, 2010−2023.
(16) Northrop, J. P.; Nguyen, D.; Piplani, S.; Olivan, S. E.; Kwan, S. T.; et al. *Mol. Endocrinol.* **2000**, *14*, 605−622.
(17) Rodriguez, A. L.; Tamrazi, A.; Collins, M. L.; Katzenellenbogen, J. A. *J. Med. Chem.* **2004**, *47*, 600−611.
(18) Parent, A. A.; Gunther, J. R.; Katzenellenbogen, J. A. *J. Med. Chem.* **2008**, *51*, 6512−6530.
(19) Sun, A.; Moore, T. W.; Gunther, J. R.; Kim, M. S.; Rhoden, E.; et al. *ChemMedChem.* **2011**, *6*, 654−666.
(20) Estébanez-Perpiñá, E.; Arnold, L. A.; Nguyen, P.; Rodrigues, E. D.; Mar, E.; et al. *Proc. Nat. Acad. Sci. U.S.A.* **2007**, *104*, 16074−16079.
(21) Gunther, J. R.; Du, Y.; Rhoden, E.; Lewis, I.; Revennaugh, B.; et al. *J. Biomol. Screening* **2009**, *14*, 181−93.
(22) Nandhikonda, P.; Lynt, W. Z.; McCallum, M. M.; Ara, T.; Baranowski, A. M.; et al. *J. Med. Chem.* **2012**, *55*, 4640−51.
(23) Arnold, L. A.; Estébanez-Perpiñá, E.; Togashi, M.; Jouravel, N.; Shelat, A.; et al. *J. Biol. Chem.* **2005**, *280*, 43048−55.
(24) Phan, T.; Nguyen, H. D.; Göksel, H.; Möcklinghoff, S.; Brunsveld, L. *Chem. Commun.* **2010**, *46*, 8207−8209.
(25) Leduc, A. M.; Trent, J. O.; Wittliff, J. L.; Bramlett, K. S.; Briggs, S. L.; et al. *Proc. Natl., Acad. Sci. U.S.A.* **2003**, *100*, 11273−11278.
(26) Geistlinger, T. R.; Guy, R. K. *J. Am. Chem. Soc.* **2003**, *125*, 6852−6853.
(27) Phillips, C.; Roberts, L. R.; Schade, M.; Bazin, R.; Bent, A.; et al. *J. Am. Chem. Soc.* **2011**, *133*, 9696−9699.
(28) Mattheakis, L. C.; Bhatt, R. R.; Dower, W. J. *Pro. Natl. Acad. Sci. U.S.A.* **1994**, *91*, 9022−9026.
(29) He, M.; Taussig, M. J. *Nat. Methods* **2007**, *4*, 281−288.
(30) Hanes, J.; Plückthun, A. *Proc. Natl. Acad. Sci. U.S.A.* **1997**, *94*, 4937−4942.
(31) Yang, L. M.; Wang, J. L.; Kang, L.; Gao, S.; Liu, Y. H.; Hu, T. M. *PLoS One* **2008**, *3*, e2092.
(32) Bramlett, K. S.; Wu, Y.; Burris, T. P. *Mol. Endocrinol.* **2001**, *15*, 909−922.
(33) Doig, A. J. The α-Helix as the Simplest Protein Model: Helix−Coil Theory, Stability, and Design. In *Protein Folding, Misfolding and Aggregation: Classical Themes and Novel Approaches*; Muñoz, V., Ed.; RSC Publishing: Cambridge, U.K., 2008; pp 1−27.
(34) Luo, P.; Baldwin, R. L. *Biochemistry* **1997**, *36*, 8413−8421.
(35) Plevin, M. J.; Mills, M. M.; Ikura, M. *Trends Biochem. Sci.* **2005**, *30*, 66−69.
(36) Sherman, M. P.; De Noronah, C. M. C.; Pearce, D.; Greene, W. C. *J. Virol.* **2000**, *74*, 8159−8165.
(37) Landschulz, W. H.; Johnson, P. F.; McKnight, S. L. *Science* **1988**, 1759−1764.
(38) Van Arnam, E. B.; Lester, H. A.; Dougherty, D. A. *ACS Chem. Biol.* **2011**, *6*, 1063−1068.
(39) Viguera, A. R.; Serrano, L. *Protein Sci.* **1999**, *8*, 1733−1742.
(40) Prieto, J.; Serrano, L. *J. Mol. Biol.* **1997**, *274*, 276−288.
(41) Kumar, S.; Bansal, M. *Proteins: Struct., Funct., Genet.* **1998**, *31*, 460−476.

(42) Andrews, M. J. I.; Tabor, A. B. *Tetrahedron* **1999**, *55*, 11711−11743.
(43) Gregor, C. R.; Cerasoli, E.; Tulip, P. R.; Ryadnov, M. G.; Martyna, G. J.; Crain, J. *Phys. Chem. Chem. Phys.* **2011**, *13*, 127−135.
(44) Zimm, B. H.; Bragg, J. K. *J. Chem. Phys.* **1959**, *31*, 526−535.
(45) Lifson, S.; Roig, A. *J. Chem. Phys.* **1961**, *34*, 1963−1974.
(46) MacArthur, M. W.; Thornton, J. M. *J. Mol. Biol.* **1991**, *218*, 397−412.
(47) McInerney, E. M.; Rose, D. W.; Flynn, S. E. *Genes Dev.* **1998**, *12*, 3357−3368.
(48) Mettu, N. B.; Stanley, T. B.; Dwyer, M. A.; Jansen, M. S.; Allen, J. E.; et al. *Mol. Endocrinol.* **2007**, *21*, 2361−2377.
(49) Yang, J.; Chang, C.; Safi, R.; Morgan, J.; McDonnell, D. P.; et al. *Mol. Endocrinol.* **2011**, *25*, 32−43.
(50) Dominguez Seoane, M.; Petkau-Milroy, K.; Vaz, B.; Möcklinghoff, S.; Folkertsma, S.; et al. *Med. Chem. Commun.* **2013**, *4*, 187−192.
(51) Kay, B. K.; Williamson, M. P.; Sudol, M. *FASEB J.* **2000**, *14*, 231−241.
(52) Geistlinger, T. R.; McReynolds, A. C.; Guy, R. K. *Chem. Biol.* **2004**, *11*, 273−281.
(53) Rachez, C.; Gamble, M.; Chang, C. P.; Atkins, G. B.; Lazar, M. A.; Freedman, L. P. *Mol. Cell. Biol.* **2000**, *20*, 2718−2726.
(54) Pogenberg, V.; Guichou, J. F.; Vivat-Hannah, V.; Kammerer, S.; Pérez, E.; et al. *J. Biol. Chem.* **2005**, *280*, 1625−1633.
(55) Lee, J. W.; Choi, H. S.; Gyuris, J.; Brent, R.; Moore, D. D. *Mol. Endocrinol.* **1995**, *9*, 243−254.
(56) Malovannaya, A.; Lanz, R. B.; Jung, S. Y.; Bulynko, Y.; Le, N. T.; et al. *Cell* **2011**, *145*, 787−799.
(57) Vanhooke, J. L.; Benning, M. M.; Bauer, C. B.; Pike, J. W.; DeLuca, H. F. *Biochemistry* **2004**, *43*, 4101−4110.